





Line-field confocal optical coherence tomography for actinic keratosis and squamous cell carcinoma: a descriptive study

E. Cinotti,¹  L. Tognetti,¹ A. Cartocci,² A. Lamberti,¹  S. Gherbassi,¹ C. Orte Cano,³ C. Lenoir,³ G. Dejonckheere,³ G. Diet,³ M. Fontaine,³ M. Miyamoto,³ J. Perez-Anker,^{4,5}  V. Solmi,¹ J. Malveyh,^{4,5} V. del Marmol,³ J. L. Perrot,⁶ P. Rubegni¹ and M. Suppa^{3,7} 

¹Dermatology Unit, Department of Medical, Surgical and Neurological Sciences, University of Siena, Siena, Italy; ²Department of Medical Biotechnologies, University of Siena, Siena, Italy; ³Department of Dermatology, Hôpital Erasme, Université Libre de Bruxelles, Brussels, Belgium; ⁴Melanoma Unit, Hospital Clinic Barcelona, University of Barcelona, Barcelona, Spain; ⁵CIBER de Enfermedades Raras, Instituto de Salud Carlos III, Barcelona, Spain; ⁶Department of Dermatology, University Hospital of Saint-Etienne, Saint-Etienne, France; and ⁷Department of Dermatology, Institut Jules Bordet, Université Libre de Bruxelles, Brussels, Belgium

doi:10.1111/ced.14801

Summary

Background. Early and accurate diagnosis of cutaneous squamous cell carcinomas (SCCs) and actinic keratoses (AK) is fundamental to reduce their associated morbidity and to select the correct treatment. Line-field confocal optical coherence tomography (LC-OCT) is a new imaging device that can characterize healthy skin and basal cell carcinoma, but no large studies on keratinocyte cell tumours have yet been published.

Aim. To identify and describe LC-OCT criteria associated with SCC and AK, and to compare LC-OCT findings in these tumours.

Methods. A retrospective observational multicentre study was conducted. Lesions were imaged with the LC-OCT device before surgery and examined histologically. LC-OCT criteria for AK/SCC were identified and their presence was evaluated in all study lesions. Univariate and multivariate analyses were performed to compare AK and SCCs, and to investigate differences between *in situ* and invasive tumours.

Results. In total, 158 patients with 50 AK and 108 SCCs (62 *in situ* and 46 invasive) were included. Cytological and architectural alterations were found in most lesions, and differences were found between AK and SCCs. Although the visualization of the dermoepidermal junction (DEJ) was often hampered by hyperkeratosis and acanthosis, an outlined DEJ without broad strands was observed in almost all AK and almost all *in situ* SCCs, but in only three invasive SCCs ($P < 0.001$) when the DEJ was detectable.

Conclusion. Our results suggest that LC-OCT can help clinicians in the identification of AK and SCC and their differentiation, providing a real-time and noninvasive examination. Further studies are needed to confirm our data.

Introduction

Cutaneous squamous cell carcinoma (SCC) is the second most frequent cancer in humans. Although it usually exhibits benign clinical behaviour, it can be both locally invasive with high morbidity or metastatic with high mortality.^{1,2} Actinic keratoses (AK) are precancerous lesions that can progress into SCC.^{3,4} They represent an important issue in dermatological practice because their prevalence is rising as a result of increasing life

Correspondence: Dr Elisa Cinotti, Dermatology Unit, Department of Medical, Surgical and Neurological Sciences, University of Siena, Viale Bracci 16, Siena, 53100, Italy
E-mail: elisacinotti@gmail.com

Conflict of interest: the authors declare that they have no conflicts of interest.

Accepted for publication 10 June 2021

expectancy and prolonged sun exposure.^{5,6} Bowen disease (BD) is an intraepidermal SCC with a particular pathogenesis and clinicopathological features, which rarely progresses to invasive SCC and shows histological similarities to bowenoid AK grade III, based on the R wert-Huber classification.^{7,8} Early and accurate diagnosis of AK and SCC and identification of SCC invasiveness is necessary for correct treatment choice, particularly as AK can be treated with noninvasive treatments whereas invasive SCC needs surgical excision.^{9–11}

Although histological examination remains the gold standard for diagnosis, there is an increasing interest in noninvasive imaging technologies in this field, both for diagnosis and for follow-up after noninvasive treatments.⁴ Indeed, since AK are often multiple in a field of cancerization, multiple biopsies would be needed but they would be deleterious in terms of time, cost and aesthetic outcome.¹² Additionally, noninvasive skin imaging could also guide biopsies.

Dermoscopy is currently used in clinical practice to help with the correct classification of keratinocyte skin tumours.^{13–16} However, correct classification based only on clinical and dermoscopic data can be challenging, and large studies on clinical and dermoscopic diagnostic accuracy for the differentiation of AK and SCC are lacking. Moreover, this technique cannot recognize subclinical AK within a field of cancerization.

Additional noninvasive tools such as reflectance confocal microscopy (RCM), conventional optical coherence tomography (OCT) and high-definition (HD)-OCT provide information that is closer to that obtained by histological examination, and have been investigated in terms of diagnostic performance for both clinical and subclinical keratinocyte skin tumours.^{4,12} Dedicated Cochrane Reviews found insufficient evidence for the use of RCM or OCT for the diagnosis of SCC.^{17–19} OCT can show the destruction of the epidermal/dermal layering in keratinocyte skin tumours but does not have sufficient resolution to identify single keratinocytes and to clearly identify keratinocyte tumour proliferation.²⁰ Although RCM has a higher lateral resolution than conventional OCT (1 μm vs. 7.5 μm) and can detect cellular changes,^{16,21} it has a lower penetration (~200 μm vs. 1–2 mm) that can prevent visualization of the dermoepidermal junction (DEJ) in hyperkeratotic lesions, and RCM only provides horizontal skin sections, in which it is more difficult to define tumour invasiveness and to discriminate AK from SCC than with conventional OCT.^{12,20} HD-OCT seemed to overcome the problems of both the previous techniques by providing images with cellular resolution (isotropic resolution 3 μm), good penetration (~570 μm) and vertical sections.^{22–25} However,

even though the device was found to be promising for the diagnosis of cutaneous carcinomas including AK and SCC,^{22,23} the difficulty in handling it due to its large size and weight led to its withdrawal from the market.

Recently, a new technology has been developed, named line-field confocal (LC)-OCT, which has far superior technical characteristics compared with HD-OCT, having a higher cell resolution (slightly greater than 1 μm , similar to RCM) with an analogue penetration depth (~500 μm).²⁶ Moreover, it is lighter and easier to handle and has user-friendly software. Therefore, higher diagnostic accuracy for AK and SCC and easier use in clinical practice compared with previous OCT technologies can be expected. Recent studies have shown that LC-OCT can clearly identify different skin structures including single epidermal cells and the DEJ in healthy skin.²⁷ Moreover, it can reveal the cleavage level in autoimmune bullous disorders,²⁸ and it could aid the diagnosis of basal cell carcinoma (BCC),²⁹ melanocytic tumours,^{30,31} vascular tumours,³² skin infections,^{33,34} genetic disorders^{35,36} and diseases characterized by altered keratinization.³⁷

LC-OCT seems to be promising for the identification of keratinocyte tumours and their invasiveness,¹² but no large studies are yet available for AK and SCC. In this study, we aimed to describe which features can be observed using LC-OCT in AK and SCC, and to investigate any possible differences between these two tumours.

Methods

The study was conducted in accordance with the ethical principles of the Helsinki Declaration. All patients gave informed consent for their images to be anonymously used in this study.

Study lesions

SCCs and AK were collected from the databases of the Dermatology Departments of the Erasme University Hospital of Brussels (Belgium) and the University Hospital of Siena (Italy). The time frame of the inclusion ranged from 1 August 2018 to 30 September 2020 in Brussels and from 1 February 2020 to 30 September 2020 in Siena. All lesions were excised and histopathologically confirmed.

Line-field confocal optical coherence tomography device

LC-OCT is a time-domain OCT technology that uses line illumination of the skin and line detection of the

signal rather than point scanning/detection. In this study, an LC-OCT device producing B-scans (vertically-orientated sectional images and videos) was used. Images/videos were acquired with a CE-marked prototype LC-OCT (DAMAE Medical, Paris, France) by two investigators (EC and MS) expert in skin imaging. The device is composed of a handheld probe connected to a central unit and a display. The device has 1.1- μm axial resolution, 1.3- μm lateral resolution, 500- μm scanning depth, 1.2-mm lateral field of view and 10 frames/second acquisition.²⁶

Image acquisition protocol

A drop of paraffin oil was placed between the lesion and the glass window at the tip of the LC-OCT camera to ensure refractive index matching. Live images were directly visualized on the screen, while the operator gently moved the tip of the probe over the lesion. At least four LC-OCT images and two videos were saved for each lesion.

Image evaluation

The LC-OCT criteria were chosen based on previously described histological, RCM, conventional OCT and HD-OCT criteria for AK and SCC,^{20–23} and the expert opinion of the authors (Table 1). Three observers (EC, LT and AL) blinded to any clinical, dermoscopic and histopathological data retrospectively evaluated all study lesions for LC-OCT image quality (good or poor based on the visibility of the cells and the different skin layers) and the presence/absence of each LC-OCT criterion. The thicknesses were measured using the ruler provided by the machine software. Any disagreement was solved by consensus among the evaluators.

Statistical analysis

We calculated the frequencies of qualitative variables and mean \pm SD for quantitative variables. The association between qualitative variables and the outcome was evaluated by Fisher exact test for a 2×2 contingency table or χ^2 for the other cases. We used *t*-test (AK/SCC outcome) or ANOVA (AK/*in situ* SCC/invasive SCC, or BD/*in situ* SCC other than BD) if the variables were normally distributed (as evaluated by Kolmogorov–Smirnov test) and there was homoscedasticity between variances (evaluated by Bartlett test), otherwise Mann–Whitney or Kruskal–Wallis test was used. Logistic regression was later performed to evaluate variables that were statistically significant at the

Table 1 Description of line-field confocal optical coherence tomography criteria for actinic keratosis and squamous cell carcinoma (based on literature review and expert opinion).

LC-OCT criteria	Definition
Hyperkeratosis	Stratum corneum thickness > 20 μm
Parakeratosis	Small dark areas corresponding to cell nuclei inside the stratum corneum
Erosion, ulceration	Dark areas with sharp borders and irregular contours filled with amorphous material, cellular debris and small particles
Acanthosis	Epidermal thickness > 60 μm
Disarranged epidermal architecture	Variation in shape and size of epidermal nuclei of keratinocytes and variation in reflectivity of keratinocytes; the normal architecture of the epidermis with its well-defined different layers is no longer visible
Dyskeratotic keratinocytes	Large hyper-reflective round cells inside the epidermis
Atypical nuclei	Nuclei are irregular in shape and size
Crowded nuclei	High density of keratinocyte nuclei
Mottled pigmentation of keratinocytes	Presence of clustered hyper-reflective keratinocytes
Pigmentation of the basal layer	Hyper-reflective basal layer of the epidermis
Keratin pearls	Whorl-shaped accumulation of keratin, appearing as a dark area with hyper-reflective and undulated lines
Whorled appearance	Whorled arrangement of keratinocyte nuclei inside the epidermis
Dermoepidermal junction	Well-defined homogeneous hyporeflective small band separating the epidermis from the dermis, which can be linear or jagged. It was defined as outlined when it was not interrupted by tumour proliferations
Adnexal involvement	Enlarged hair-follicle epithelium with nuclei of irregular shape and size
Tumour budding	Rounded projection of a completely disarranged epidermis, composed of atypical keratinocytes with blurred outline
Broad strands	Invasive strands of atypical and dyskeratotic keratinocytes interrupting the dermoepidermal junction and projecting irregularly into the dermis
Dilated linear vessels	Large, well-defined hyporeflective elongated areas in the dermis characterized by the flowing of blood cells in the LC-OCT video
Glomerular vessels	Hyporeflective, loosely packed and spiral-shaped blood vessels within the superficial dermis
Elastosis	Hyporeflective areas in the dermis

LC-OCT, line-field confocal optical coherence tomography.

previous univariate analysis. The best subset of variables was selected by a stepwise procedure based on the Akaike information criterion. OR and 95% CI were

estimated by logistic regression. All statistical tests were two-tailed and $P < 0.05$ was considered statistically significant. The analyses were carried out by R software (V3.6.2; <https://www.r-project.org/>).

Results

Clinical features

In total, 158 patients (83 women, 75 men; median \pm SD age 69.8 ± 12.7 years, range 34–95 years) with 158 lesions were enrolled in the study. The majority (88.0%) of patients attended the Erasme University Hospital of Brussels (Belgium) and 12.0% attended the University Hospital of Siena (Italy). The 158 histopathologically proven tumours comprised 50 AK and 108 SCCs (Table 2). Of the 108 SCCs, 62 were *in situ* and 46 were invasive; of the 62 *in situ* tumours, 25 were BD. No Bowenoid AK grade III according to R wert-Huber⁸ was found.

The majority of SCCs were located on the head/neck region (54.6%), followed by the legs (17.6%), arms (14.8%) and trunk (13.0%). Similarly, AK were mainly located on the head/neck region (62.0%), followed by the legs (14.0%), arms (12.0%) and trunk (12.0%). No statistically significant differences in sex, age or body location were found between AK and SCC.

Univariate analysis of line-field confocal optical coherence tomography features

LC-OCT images were considered of good quality in 76.0% of AK and 73.1% of SCC cases (Table 3). Comparison of BD and *in situ* SCC other than BD could not find any differences, except for dyskeratotic keratinocytes, which were less frequently found in BD

($P = 0.04$, marginally significant value). Therefore, BD was pooled with *in situ* SCCs for the comparison with AK and invasive SCC to improve the statistical power of the analyses.

The epidermis was easily visible in most cases (95.9% of AK and 88.8% of SCCs). Higher values were found in SCC than in AK for minimum, maximum and mean lesion thickness without the stratum corneum ($P < 0.001$ for all) and for the mean thickness of the stratum corneum ($P = 0.02$). Hyperkeratosis was more frequent in SCC than in AK ($P = 0.02$), whereas parakeratosis, erosion/ulceration and acanthosis were similarly distributed across the two entities.

Most tumours [84.0% of AK (Figs 1, S1 and 2) and 91.7% of SCCs (Figs 3–6)] had at least one of the following criteria: disarranged epidermal architecture, dyskeratotic keratinocytes and atypical nuclei. The epidermal architecture was significantly ($P = 0.01$) more frequently disarranged in SCC (94.0%) than in AK (77.8%), while dyskeratotic keratinocytes were present in most AK (82.2%) and SCCs (72.3%). The nuclei of keratinocytes were visible in almost all cases (96.0% of AK and 95.3% of SCCs) and the nuclei were atypical in most cases (87.2% of AK and 91.3% of SCCs), while crowded nuclei were observed in about half of the cases (50.0% of AK and 47.0% of SCCs).

Keratin pearls were not observed, whereas a whorled appearance of the epidermis was noticed in only two of the *in situ* SCCs. Mottled pigmentation of the keratinocytes and hyperpigmentation of the basal layer of the epidermis were never observed.

The DEJ was not always very visible: in 18.0% AK and 25.0% SCCs the images did not contain the DEJ, whereas in 34.0% AK and 34.3% SCCs the DEJ was not well defined. Outlined DEJ was consistent with histopathology in most cases, and allowed distinction

Table 2 Demographics and clinical features of the study lesions.

	AK (N = 50)	SCC (N = 108)	P^a	<i>In situ</i> SCC (N = 62)	Invasive SCC (N = 46)	P^b
Sex, n (%)						
Female	25 (50.0)	58 (53.7)	0.73	33 (53.2)	25 (54.3)	0.90
Male	25 (50.0)	50 (46.3)		29 (46.8)	21 (45.7)	
Age, years ^c	70.7 \pm 10.9	69.3 \pm 13.5	0.53	69.3 \pm 12.6	69.5 \pm 14.7	0.82
Body location, n (%)						
Head/neck	31 (62.0)	59 (54.6)	0.82	38 (61.3)	21 (45.7)	0.29
Trunk	6 (12.0)	14 (13.0)		9 (14.5)	5 (10.9)	
Arms	6 (12.0)	16 (14.8)		9 (14.5)	7 (15.2)	
Legs	7 (14.0)	19 (17.6)		6 (9.7)	13 (28.3)	

AK, actinic keratoses; SCC, squamous cell carcinoma. ^aComparison between AK and SCC; ^bcomparison between AK, *in situ* SCC and invasive SCC; ^cmean \pm SD.

Table 3 Distribution of LC-OCT criteria across study lesions.

Parameter ^a	AK (N = 50)	SCC (N = 108)	P ^b	<i>In situ</i> SCC excluding BD (N = 37)	BD (N = 25)	P ^c	<i>In situ</i> SCC (N = 62)	Invasive SCC (N = 46)	P ^d
Good image quality	38 (76.0)	79 (73.1)	0.85	27 (73.0)	18 (72.0)	1.00	45 (72.6)	34 (73.9)	0.99
Visualization of epidermis	47 (95.9)	95 (88.8)	0.23	35 (94.6)	21 (87.5)	0.39	56 (91.8)	39 (84.8)	0.18
Lesion thickness ^e									
Minimum ^f	69 ± 41	106 ± 49	< 0.001	107 ± 48	93 ± 44	0.36	102 ± 46	113 ± 52	< 0.001 ^{g,h}
Maximum visible ^f	153 ± 71	214 ± 53	< 0.001	214 ± 62	206 ± 58	0.603	211 ± 60	217 ± 42	< 0.001 ^{g,h}
Mean ^f	105 ± 50	150 ± 49	< 0.001	152 ± 50	141 ± 46	0.486	148 ± 49	154 ± 49	< 0.001 ^{g,h}
Thickness ^f									
Minimum	18 ± 12	24 ± 20	0.06	23 ± 20	21 ± 11	0.747	22 ± 17	27 ± 23	0.07
Maximum visible	96 ± 94	103 ± 89	0.25	99 ± 95	84 ± 44	0.407	94 ± 80	116 ± 99	0.39
Mean	38 ± 33	54 ± 60	0.02	50 ± 65	52 ± 58	0.917	51 ± 62	57 ± 58	0.04 ^h
Hyperkeratosis	24 (48.0)	77 (71.3)	0.01	24 (64.9)	19 (76.0)	0.40	43 (69.4)	34 (73.9)	0.02 ^{g,h}
Parakeratosis	20 (64.5)	52 (62.7)	0.85	17 (65.4)	12 (60.0)	0.76	29 (63.0)	23 (62.2)	0.98
Erosion, ulceration	30 (61.2)	66 (62.9)	0.86	24 (68.6)	13 (56.5)	0.40	37 (61.7)	29 (64.4)	0.94
Acanthosis	38 (76.0)	77 (71.3)	0.57	31 (83.8)	16 (64.0)	0.13	47 (75.8)	30 (65.2)	0.44
Disarranged epidermal architecture	35 (77.8)	95 (94.0)	0.01	33 (94.3)	22 (91.7)	0.57	55 (93.2)	40 (95.2)	0.02 ^{g,h}
Dyskeratotic keratinocytes	37 (82.2)	73 (72.3)	0.22	30 (83.3)	14 (58.3)	0.04	44 (73.3)	29 (70.7)	0.41
Visible nuclei	48 (96.0)	102 (95.3)	0.99	36 (97.3)	24 (96.0)	1.00	60 (96.8)	42 (93.3)	0.86
Atypical nuclei	41 (87.2)	94 (91.3)	0.56	31 (86.1)	22 (91.7)	0.69	53 (88.3)	41 (95.3)	0.38
Crowded nuclei	23 (50.0)	47 (47.0)	0.86	16 (44.4)	13 (56.5)	0.42	29 (49.2)	18 (43.9)	0.83
Features of epidermal dysplasia ^l	42 (84.0)	99 (91.7)	0.17	34 (91.9)	23 (92.0)	1.00	57 (91.9)	42 (91.3)	0.4
Whorled appearance	0	2 (2.0)	0.99	0 (0.0)	2 (8.3)	0.17	2 (3.4)	0	0.34
Visible DEJ	24 (48.0)	44 (40.7)	0.40	17 (45.9)	10 (40.0)	0.79	27 (43.5)	17(37.0)	0.56
Outlined DEJ	23 (46.0)	22 (20.4)	0.01	13 (35.1)	6 (24.0)	0.41	19 (30.7)	3(6.5)	< 0.001 ^{h,i}
Adnexal involvement	21 (47.7)	31 (36.5)	0.26	13 (40.6)	8 (40.0)	1.00	21 (40.4)	10 (30.3)	0.30
Tumour budding	19 (45.2)	31 (40.8)	0.7	11 (39.3)	5 (33.3)	0.75	16 (37.2)	15 (45.5)	0.7
Broad strands	1 (3.2)	26 (38.8)	< 0.001	0 (0.0)	3 (25.0)	0.05	3 (9.7)	23 (63.9)	< 0.001 ^{h,i}
Dilated linear vessels	35 (77.8)	53 (56.4)	0.02	21 (61.8)	11 (50.0)	0.41	32 (57.1)	21 (55.3)	0.05
Glomerular vessels	37 (78.7)	61 (66.3)	0.17	24 (70.6)	13 (61.9)	0.56	37 (67.3)	24 (64.9)	0.30
Elastosis	11 (26.2)	9 (12.3)	0.08	5 (19.2)	2 (10.0)	0.45	7 (15.2)	2 (7.4)	0.12

AK, actinic keratoses; BD, Bowen disease; DEJ, dermoepidermal junction; SCC, squamous cell carcinoma. ^aData are n (%) unless otherwise indicated. Percentages were calculated on the total of the evaluable cases; numbers did not always add up to the total of AK and SCCs because of missing values (criteria were not evaluated in case of poor image quality and/or focal visualization of the corresponding skin layer). ^bComparison between AK and SCC; ^ccomparison between BD and SCC *in situ* excluding BD; ^dcomparison between AK, *in situ* SCC (including BD) and invasive SCC; ^eexcluding stratum corneum, μm; ^fmean ± SD; statistically significant values are reported for the comparison between ^gAK and *in situ* SCC, ^hAK and invasive SCC, and ⁱ*in situ* SCC and invasive SCC. ^lLesions were considered as having features of epidermal dysplasia if at least one criterion among disarranged epidermal architecture, dyskeratotic keratinocytes and atypical nuclei was found.

of AK and *in situ* SCCs from invasive SCCs. Adnexal involvement was observed in 47.7% of AK and 36.5% of SCCs. Tumour budding was visible in about half of AK and SCCs, whereas broad strands were significantly ($P < 0.001$) more frequent in invasive SCCs (63.9%) than in AK (3.2%) or *in situ* SCCs (9.7%). Dilated vessels, either glomerular or linear, were found in most cases; dilated linear vessels were significantly ($P = 0.02$) more frequent in AK (77.8%) than in SCC

(56.4%). Elastosis was observed in a small portion of cases (26.2% of AK and 12.3% of SCC).

Multivariate analysis of line-field confocal optical coherence tomography features

Final logistic regression model obtained by the analysis of the LC-OCT variables that were statistically significant in univariate analysis showed that disarranged

Figure 1 (a–d) Actinic keratosis: (a) dermoscopic, (b) histopathological and (c,d) line-field confocal optical coherence tomography (LC-OCT) images. (b) Histopathological examination shows mild keratinocyte atypia in the epidermis and prominent hair follicles (white star). (c,d) LC-OCT examination reveals the presence of atypical keratinocyte nuclei inside the epidermis (red asterisk) and a well-outlined dermoepidermal junction (DEJ, red arrow). (c) A hair follicle is also present (white star). Scale bar = 100 μ m.

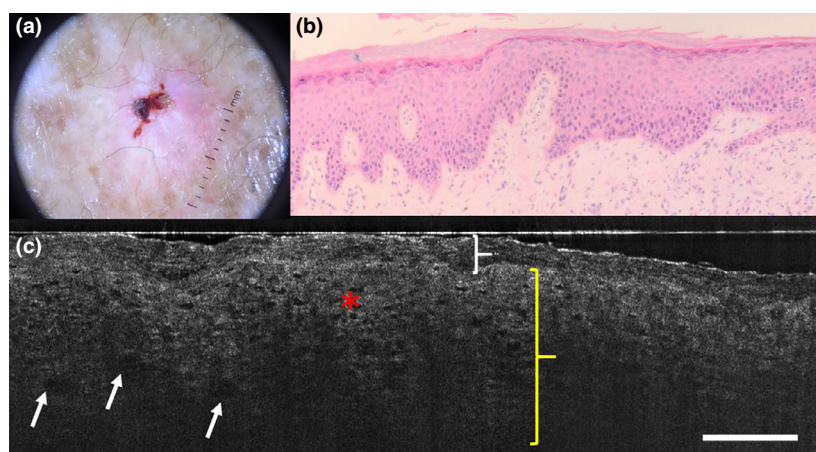
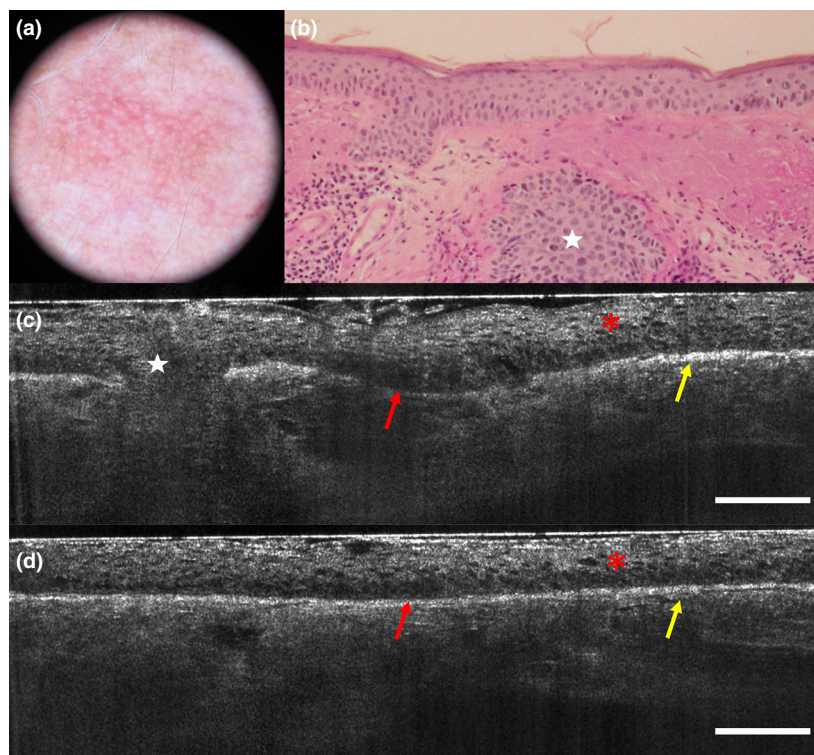


Figure 2 (a–c) Actinic keratosis: (a) dermoscopic, (b) histopathological and (c) line-field confocal optical coherence tomography (LC-OCT) images. (c) LC-OCT examination reveals the presence of hyperkeratosis (white brace), acanthosis (yellow brace) and atypical nuclei of keratinocytes inside the epidermis (red asterisk). The dermoepidermal junction is not visible. Roundish hyporeflective areas corresponding to glomerular vessels are discernible (white arrow). Scale bar = 100 μ m.

epithelial architecture (OR = 5.24, 95% CI 1.13–24.39; $P = 0.04$), maximum visible lesion thickness (OR = 1.02 for every μ m increase in thickness, 95% CI 1.01–1.03; $P < 0.001$) and broad strands (OR = 8.6, 95% CI 1.49–164.63; $P = 0.04$) were indicative of SCC.

Discussion

Our study describes the LC-OCT features of keratinocyte tumours and shows that LC-OCT is able to identify major features of AK and SCC that can help distinguish between these two conditions.

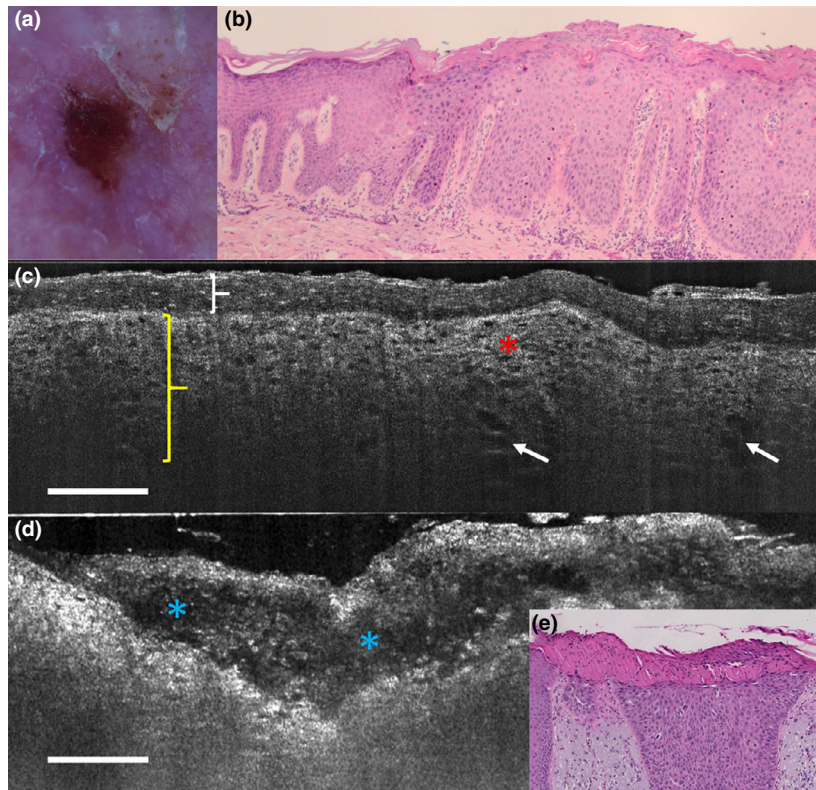


Figure 3 (a–d) Squamous cell carcinoma *in situ* (Bowen subtype): (a) dermoscopic, (b) histopathological and (c,d) line-field confocal optical coherence tomography (LC-OCT) images. (c) LC-OCT examination reveals the presence of hyperkeratosis (white brace), acanthosis (yellow brace), atypical nuclei of keratinocytes inside the epidermis (red asterisk) and roundish hyporeflective areas corresponding to glomerular vessels (white arrow). The dermoepidermal junction is not visible. (d) An erosion with an overlying crust (blue asterisk) is detectable and correlates with (e) histological image. Scale bar = 100 µm.

Discrimination from normal skin also seems to be feasible, as hyperkeratosis, acanthosis, parakeratosis, erosion/ulceration, disarranged epithelial architecture, dyskeratotic keratinocytes, crowded nuclei, atypical nuclei, tumour budding and dilated vessels were prominent features of both AK and SCCs. Moreover, nonoutlined DEJ and broad strands characterized invasive tumours. Additional features were also revealed by the device, such as the involvement of hair-follicle epithelium and presence of solar elastosis. Notably, at least one of the three criteria (disarranged epithelial architecture, dyskeratotic keratinocytes, and atypical nuclei) was present in most lesions, therefore, these represent major criteria characterizing AK and SCC under LC-OCT. Disarranged epithelial architecture reflects a loss of orderly keratinocyte maturation, while dyskeratotic keratinocytes indicate altered keratinization processes. The nuclei of keratinocytes are visible as well-demarcated hyporeflective oval areas under LC-OCT, and their irregularity in shape and size, scored as ‘atypical nuclei’, can be considered as an indirect sign of keratinocyte pleomorphism when using the LC-OCT device employed in this study (two-dimensional imaging in the vertical plane). More direct evaluation of keratinocyte pleomorphism can be obtained with more

recent and advanced LC-OCT devices, which are able to assess the skin in a three-dimensional (3D) fashion (imaging in both the vertical and horizontal plane, 3D skin reconstructions).

Interestingly, LC-OCT was able to provide images of good quality in three-quarters of the cases we studied, despite the presence of a thick stratum corneum, which could have caused possible alteration of the imaging signal. It should be highlighted that in our study the lesions were not selected, and thus images of all types of tumours, including clinically hyperkeratotic tumours, were included. Hyperkeratosis produces excessive hyper-reflectivity of the upper part of the lesions and reduces image quality of the underlying layers of the skin for LC-OCT as it does for RCM.³⁸ In future, it could be interesting to image hyperkeratotic lesions following superficial curettage or previous application of a keratolytic cream. Hyperkeratosis and acanthosis limited visualization of the DEJ, especially in SCC, for which it was not possible to reach the DEJ in a quarter of cases.

Compared with AK, SCCs have significantly higher mean thickness both for the lesion ($P < 0.001$) and the stratum corneum ($P = 0.02$), and the finding of disarranged epidermal architecture was more frequent ($P = 0.01$). Interestingly, differences between AK and

Figure 4 (a–c) Squamous cell carcinoma *in situ* (Bowen subtype): (a) dermoscopic, (b) histopathological and (c) line-field confocal optical coherence tomography (LC-OCT) images. (c) LC-OCT examination reveals the presence of hyperkeratosis (white brace), acanthosis (yellow brace) and atypical keratinocyte nuclei irregular in size and shape inside the epidermis (red asterisk). The dermoepidermal junction is also visible (red arrow). Roundish hyporeflexive areas corresponding to glomerular (white arrow) and linear (light blue arrow) vessels are discernible. Scale bar = 100 μ m.

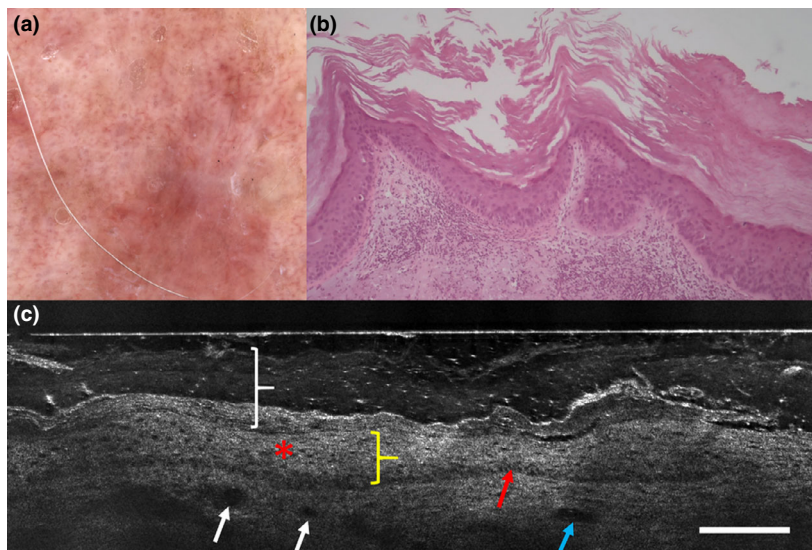
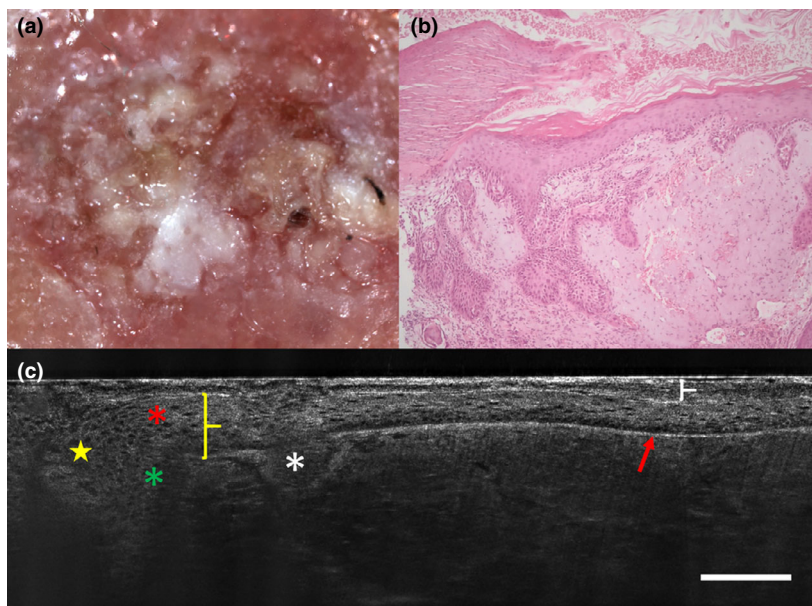


Figure 5 (a–c) Microinvasive squamous cell carcinoma: (a) dermoscopic, (b) histopathological and (c) line-field confocal optical coherence tomography (LC-OCT) images. (c) LC-OCT examination reveals the presence of hyperkeratosis (white brace), acanthosis (yellow brace), atypical nuclei of keratinocyte (red asterisk) and tumour budding (white arrow). Adnexal involvement is present (yellow star). The dermoepidermal junction is well outlined (red arrow), except in focal areas (green asterisk). Scale bar = 100 μ m.



SCC in minimum, maximum and mean lesion thickness, hyperkeratosis and disarranged epidermal architecture were independent of SCC subtype (*in situ* or invasive), whereas the mean thickness of the stratum corneum was higher in invasive SCCs than in AK. Multivariate analysis confirmed that the probability of the tumour being SCC significantly increased by 2% for each μ m of increment in lesion thickness.

A nonoutlined DEJ has been described as a highly accurate morphological OCT feature to distinguish SCC from AK, and appears to be related to irregular broad strands of the epidermis protruding into the upper dermis and/or the presence of periadnexal collars

penetrating through the DEJ.²² In about half the cases in our series, the DEJ was either not present or not very visible, probably due to hyperkeratosis and acanthosis. The LC-OCT device can scan down to a depth of 500 μ m, but the image definition degrades with increasing depth, and hyperkeratosis increases the imaging noise. Despite these limitations, when the DEJ was clearly detectable, it was outlined in all but two *in situ* lesions, but in only three invasive SCCs. Despite the small numbers in the study (probably justifying the large CI found in our multivariate analysis), broad strands were highly suggestive of SCC; when observed in AK, they probably corresponded to hair follicles or

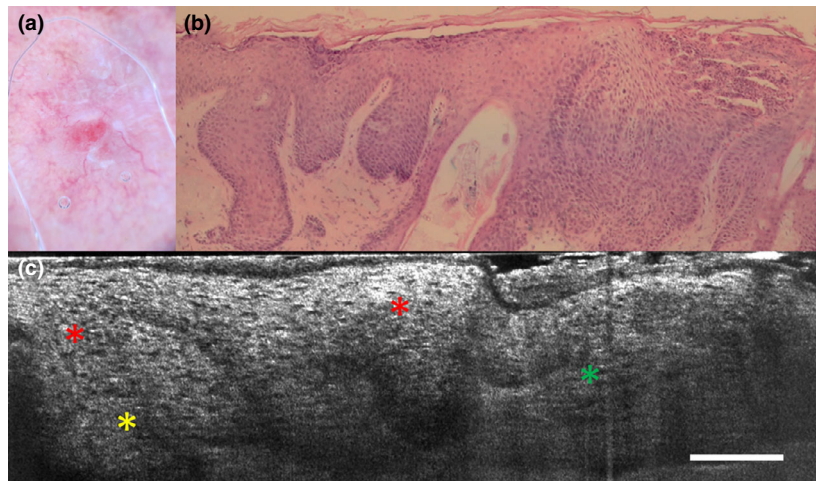


Figure 6 (a–c) Invasive squamous cell carcinoma: (a) dermoscopic, (b) histopathological and (c) line-field confocal optical coherence tomography (LC-OCT) images. (c) LC-OCT examination reveals the presence of atypical keratinocyte nuclei irregular in size and shape inside the epidermis (red asterisk). The dermoepidermal junction is not well outlined (green asterisk) and tumour broad strands (yellow asterisk) are visible. Scale bar = 100 μm .

basal proliferation (PRO-III grade),³⁹ which could be challenging to distinguish from invasive SCC. Misclassification of hair follicles can probably be overcome in clinical practice by the real-time image acquisition, which allows distinction of tumour strands from hair follicles, as the hyper-reflective hair shaft can be seen moving gently underneath the camera. The correct definition of the DEJ outline enabled us to distinguish AK and *in situ* SCC from invasive tumours. It should be noted that, although the parameter ‘outlined DEJ’ was not evaluated in some SCCs because the DEJ was not sufficiently visible, this altered visibility could itself be an intrinsic characteristic of SCCs and could characterize the nonoutlined DEJ. Therefore, it would be interesting in future studies to better define the nonoutlined DEJ and to include among the evaluated criteria the interface lichenoid-like feature appearing as an undefined hyporeflective area obscuring the DEJ. Moreover, it could be useful to compare lesion thickness measured by LC-OCT and histopathology, and to compare LC-OCT data with those obtained by other noninvasive imaging techniques such as RCM.

Some features such as linear dilated vessels and elastosis had unexpectedly higher frequencies in AK than in SCC. However, prominent vessels and elastosis have been reported in AK in previous HD-OCT studies,⁴⁰ and they may have been less visible in SCC due to the thicker epidermis preventing visualization of the dermis.

This study was performed by analysing vertical sections, which are quicker to evaluate and more relevant for the identification of the DEJ. However, newer LC-OCT devices can also acquire horizontal sections and 3D images, giving the possibility of reconstruction through dedicated software. As already stated, better results might be obtained from analysis of horizontal

sections, as keratinocytes have better-defined contours than in vertical images and cell atypia can be better observed. 3D images can also enable the operator to clearly distinguish broad strands from hair follicles, a previously mentioned limitation of single-slice images. This could be further enhanced by the availability of real-time dermoscopic/LC-OCT correlations offered by the new-generation devices recently on the market.

Concerning BD, the LC-OCT features evaluated in our study did not allow us to distinguish BD tumours from other *in situ* SCCs, and further studies should be conducted to evaluate additional cytological and architectural features that could help their distinction. Moreover, as bowenoid AK grade III (Röwert-Huber classification) also shows histological similarities to BD, further studies should be conducted on this subtype of AK, which was absent in our series.

Our results from LC-OCT diagnosis of AK and SCCs are encouraging and showed that higher lesion thickness, disarranged epidermal architecture and nonoutlined DEJ could help differentiate SCC from AK. Nevertheless, some limitations of the study exist, including the retrospective design, the lack of inclusion of clinical and dermoscopic features, the lack of investigation of AK grading, and the absence of comparison with other skin tumours. Tumour lobules with a triad of colour (previously described as the major LC-OCT criteria for BCC)²⁷ were never observed in our series; their absence favours the differential diagnosis between AK/SCC and BCC, although we did not have a comparison group in the present study. Indeed, our results showed that, differently from BCC, expansion of SCC towards the dermis is characterized by tumour budding and broad strands. Moreover, the number of AK were much smaller than that of SCCs because our

study was designed to evaluate only lesions that had been examined histologically, and lesions clinically suggestive of AK are less frequently biopsied than those suggestive of SCC. Finally, the poor LC-OCT image quality in a quarter of the study cases could be regarded as another limitation; however, this was mainly related to hyperkeratosis, which represents a well-known limitation for all other noninvasive imaging techniques as well, including RCM.³⁸ In order to report real-life data, we decided to execute this study on all lesions comprised in our databases, including the hyperkeratotic ones, thus leading to the poor image quality in some of the case.

Conclusion

LC-OCT is a new noninvasive imaging technique that combines cellular resolution and visualization down to the superficial reticular dermis. It seems to be a promising tool that could help clinicians to detect the cellular and architectural alterations of keratinocyte skin tumours in real time. To our knowledge, the current study is the first to describe the LC-OCT characteristics of AK and SCCs. Our study showed that LC-OCT can identify many morphological features, such as acanthosis, hyperkeratosis, parakeratosis, erosion/ulceration, disarranged epidermal architecture, dyskeratotic keratinocytes, atypical nuclei, adnexal involvement, tumour budding, broad strands, dilated vessels and elastosis, which could potentially be useful for diagnosis of these tumours and for follow-up of noninvasive treatments. Moreover, greater lesion thickness and the presence of nonoutlined DEJ could help to differentiate SCC from AK. Further studies are needed to confirm our data.

What's already known about this topic?

- LC-OCT is a new noninvasive imaging technique that can characterize healthy skin and BCC *in vivo* thanks to its good resolution and penetration depth.
- To date, there are no large studies on the use of LC-OCT for the diagnosis of SCC and AK.

What does this study add?

- LC-OCT can identify cellular and architectural atypia in cutaneous keratinocytic tumours.

- It could also be useful for the differentiation of AK from SCC.

Acknowledgement

We thank M. Cazalas and C. Tavernier (DAMAE Medical, Paris, France) for their technical assistance with the LC-OCT device. Open Access Funding provided by Università degli Studi di Siena within the CRUI-CARE Agreement. [Correction added on 18 May 2022, after first online publication: CRUI funding statement has been added.]

References

- 1 Eigentler TK, Leiter U, Häfner H-M *et al.* Survival of patients with cutaneous squamous cell carcinoma: results of a prospective cohort study. *J Invest Dermatol* 2017; **137**: 2309–15.
- 2 Burton KA, Ashack KA, Khachemoune A. Cutaneous squamous cell carcinoma: a review of high-risk and metastatic disease. *Am J Clin Dermatol* 2016; **17**: 491–508.
- 3 Fuchs A, Marmur E. The kinetics of skin cancer: progression of actinic keratosis to squamous cell carcinoma. *Dermatol Surg* 2007; **33**: 1099–101.
- 4 Fernandez Figueras MT. From actinic keratosis to squamous cell carcinoma: pathophysiology revisited. *J Eur Acad Dermatol Venereol* 2017; **31**(Suppl): 5–7.
- 5 Neidecker MV, Davis-Ajami ML, Balkrishnan R, Feldman SR. Pharmacoeconomic considerations in treating actinic keratosis. *Pharmacoeconomics* 2009; **27**: 451–64.
- 6 Cinotti E, Perrot JL, Labeille B *et al.* Prevalence of actinic keratosis in a French cohort of elderly people: the PROOF study. *G Ital Dermatol Venereol* 2017; **152**: 537–40.
- 7 Fernández-Figueras MT, Carrato C, Sáenz X *et al.* Actinic keratosis with atypical basal cells (AK I) is the most common lesion associated with invasive squamous cell carcinoma of the skin. *J Eur Acad Dermatol Venereol* 2015; **29**: 991–7.
- 8 Røwert-Huber J, Patel MJ, Forschner T *et al.* Actinic keratosis is an early in situ squamous cell carcinoma: a proposal for reclassification. *Br J Dermatol* 2007; **156** (Suppl): 8–12.
- 9 Stratigos AJ, Garbe C, Dessinioti C *et al.* European interdisciplinary guideline on invasive squamous cell carcinoma of the skin: Part 2. Treatment. *Eur J Cancer* 2020; **128**: 83–102.
- 10 Morton CA, Szeimies R-M, Basset-Seguín N *et al.* European Dermatology Forum guidelines on topical photodynamic therapy 2019 Part 1: treatment delivery and established indications – actinic keratoses, Bowen's

- disease and basal cell carcinomas. *J Eur Acad Dermatol Venereol* 2019; **33**: 2225–38.
- 11 Heppt MV, Leiter U, Steeb T *et al.* S3 guideline for actinic keratosis and cutaneous squamous cell carcinoma – short version, part 1: diagnosis, interventions for actinic keratoses, care structures and quality-of-care indicators. *J Dtsch Dermatol Ges* 2020; **18**: 275–94.
 - 12 Dejonckheere G, Suppa M, del Marmol V *et al.* The actinic dysplasia syndrome – diagnostic approaches defining a new concept in field carcinogenesis with multiple cSCC. *J Eur Acad Dermatol Venereol* 2019; **33**: 16–20.
 - 13 Zalaudek I, Argenziano G. Dermoscopy of actinic keratosis, intraepidermal carcinoma and squamous cell carcinoma. *Curr Probl Dermatol* 2015; **46**: 70–6.
 - 14 Zalaudek I, Giacomet J, Schmid K *et al.* Dermoscopy of facial actinic keratosis, intraepidermal carcinoma, and invasive squamous cell carcinoma: a progression model. *J Am Acad Dermatol* 2012; **66**: 589–97.
 - 15 Zalaudek I, Giacomet J, Argenziano G *et al.* Dermoscopy of facial nonpigmented actinic keratosis. *Br J Dermatol* 2006; **155**: 951–6.
 - 16 Cinotti E, Labeille B, Debarbieux S *et al.* Dermoscopy vs. reflectance confocal microscopy for the diagnosis of lentigo maligna. *J Eur Acad Dermatol Venereol* 2018; **32**: 1284–91.
 - 17 Dinnes J, Deeks JJ, Chuchu N *et al.* Reflectance confocal microscopy for diagnosing keratinocyte skin cancers in adults. *Cochrane Database Syst Rev* 2018; **12**: CD013191.
 - 18 Ferrante di Ruffano L, Dinnes J, Deeks JJ *et al.* Optical coherence tomography for diagnosing skin cancer in adults. *Cochrane Database Syst Rev* 2018; **12**: CD013189.
 - 19 Valdés-Morales KL, Peralta-Pedrero ML, Cruz FJ-S, Morales-Sánchez MA. Diagnostic accuracy of dermoscopy of actinic keratosis: a systematic review. *Dermatol Pract Concept* 2020; **10**: e2020121.
 - 20 Casari A, Chester J, Pellacani G. Actinic keratosis and non-invasive diagnostic techniques: an update. *Biomedicines* 2018; **6**: 8.
 - 21 Perrot JL, Tognetti L, Habougit C *et al.* Aspect en microscopie confocale par réflectance in vivo des kératoses actiniques: reflectance confocal microscopy features of actinic keratoses. *Ann Dermatol Venereol* 2019; **146** (Suppl): IIS16–21.
 - 22 Boone M, Marneffe A, Suppa M *et al.* High-definition optical coherence tomography algorithm for the discrimination of actinic keratosis from normal skin and from squamous cell carcinoma. *J Eur Acad Dermatol Venereol* 2015; **29**: 1606–15.
 - 23 Marneffe A, Suppa M, Miyamoto M *et al.* Validation of a diagnostic algorithm for the discrimination of actinic keratosis from normal skin and squamous cell carcinoma by means of high-definition optical coherence tomography. *Exp Dermatol* 2016; **25**: 684–7.
 - 24 Boone MA, Suppa M, Marneffe A *et al.* A new algorithm for the discrimination of actinic keratosis from normal skin and squamous cell carcinoma based on in vivo analysis of optical properties by high-definition optical coherence tomography. *J Eur Acad Dermatol Venereol* 2016; **30**: 1714–25.
 - 25 Cinotti E, Labeille B, Douchet C *et al.* Dermoscopy, reflectance confocal microscopy, and high-definition optical coherence tomography in the diagnosis of generalized argyria. *J Am Acad Dermatol* 2017; **76**: S66–8.
 - 26 Dubois A, Levecq O, Azimani H *et al.* Line-field confocal optical coherence tomography for high-resolution noninvasive imaging of skin tumors. *J Biomed Opt* 2018; **23**: 1–9.
 - 27 Monnier J, Tognetti L, Miyamoto M *et al.* In vivo characterization of healthy human skin with a novel, non-invasive imaging technique: line-field confocal optical coherence tomography. *J Eur Acad Dermatol Venereol* 2020; **34**: 2914–21.
 - 28 Tognetti L, Cinotti E, Suppa M *et al.* Line field confocal optical coherence tomography: an adjunctive tool in the diagnosis of autoimmune bullous diseases. *J Biophotonics* 2021; **14**: e202000449.
 - 29 Suppa M, Fontaine M, Dejonckheere G *et al.* Line-field confocal optical coherence tomography of basal cell carcinoma: a descriptive study. *J Eur Acad Dermatol Venereol* 2021; **35**: 1099–110.
 - 30 Lenoir C, Perez-Anker J, Diet G *et al.* Line-field confocal optical coherence tomography of benign dermal melanocytic proliferations: a case series. *J Eur Acad Dermatol Venereol* 2021; **35**: e399–401.
 - 31 Ruini C, Schuh S, Sattler E, Welzel J. Line-field confocal optical coherence tomography – practical applications in dermatology and comparison with established imaging methods. *Skin Res Technol* 2021; **27**: 340–52.
 - 32 Tognetti L, Carraro A, Lamberti A *et al.* Kaposi sarcoma of the glans: new findings by line field confocal optical coherence tomography examination. *Skin Res Technol* 2021; **27**: 285–7.
 - 33 Lacarrubba F, Verzì AE, Puglisi DF, Micali G. Line-field confocal optical coherence tomography: a novel, non-invasive imaging technique for a rapid, in-vivo diagnosis of herpes infection of the skin. *J Eur Acad Dermatol Venereol* 2021; **35**: e404–6.
 - 34 Ruini C, Schuh S, Hartmann D *et al.* Noninvasive real-time imaging of mite skin infestations with line-field confocal optical coherence tomography. *Br J Dermatol* 2021; **184**: e3.
 - 35 Tognetti L, Rizzo A, Fiorani D *et al.* New findings in non-invasive imaging of aquagenic keratoderma: line-field optical coherence tomography, dermoscopy and reflectance confocal microscopy. *Skin Res Technol* 2020; **26**: 956–9.

- 36 Tognetti L, Fiorani D, Cinotti E, Rubegni P. Tridimensional skin imaging in aquagenic keratoderma: virtual histology by line-field confocal optical coherence tomography. *Int J Dermatol* 2021; **60**: e52–4.
- 37 Tognetti L, Fiorani D, Suppa M *et al.* Examination of circumscribed palmar hypokeratosis with line-field confocal optical coherence tomography: dermoscopic, ultrasonographic and histopathologic correlates. *Indian J Dermatol Venereol Leprol* 2020; **86**: 206–8.
- 38 Xiang W, Peng J, Song X *et al.* Analysis of debrided and non-debrided invasive squamous cell carcinoma skin lesions by in vivo reflectance confocal microscopy before and after therapy. *Lasers Med Sci* 2017; **32**: 211–19.
- 39 Schmitz L, Gambichler T, Gupta G *et al.* Actinic keratoses show variable histological basal growth patterns – a proposed classification adjustment. *J Eur Acad Dermatol Venereol* 2018; **32**: 745–51.
- 40 Boone M, Suppa M, Pellacani G *et al.* High-definition optical coherence tomography algorithm for discrimination of basal cell carcinoma from clinical BCC imitators and differentiation between common subtypes. *J Eur Acad Dermatol Venereol* 2015; **29**: 1771–80.

Supporting Information

Additional Supporting Information may be found in the online version of this article:

Figure S1. Histopathological examination of an actinic keratosis shows mild keratinocyte atypia in the epidermis and prominent hair follicles (the circle and line indicate sections of hair follicles).